PERGAMON

Atmospheric Environment 33 (1999) 577–589

ATMOSPHERIC ENVIRONMENT

Measurement and modeling of the dry deposition of peroxides

Brad Hall[a,*], Candis Claiborn[a], Dennis Baldocchi[b]

[a]*Department of Civil and Environmental Engineering, Washington State University, Pullman, WA, USA*
[b]*National Ocean and Atmospheric Administration, Oak Ridge, TN, USA*

Received 26 March 1998; accepted 23 July 1998

Abstract

Measurements of the dry deposition velocity (V_d) of hydrogen peroxide (H_2O_2) and total organic peroxides (ROOH) were made during four experiments at three forested sites. Details and uncertainties associated with the measurement of peroxide fluxes by the flux-gradient method are discussed. The results are compared to those predicted using a bulk-resistance model of the type commonly used in regional photochemical models. Good agreement between the H_2O_2 V_d measurements and a bulk resistance model is obtained when the model contains a zero surface resistance (R_c) and a common form for the laminar leaf-layer resistance (R_b) based on Schmidt and Prandtl numbers. In this case, a near-zero ($<5\ s\ m^{-1}$) surface resistance is confirmed for H_2O_2 within experimental uncertainties. Surface resistances for ROOH were determined to be about 10–15 $s\ m^{-1}$ over a coniferous forest and 20–40 $s\ m^{-1}$ over a deciduous forest. Higher uncertainties for ROOH prevent a detailed analysis of the differences in R_c among forest types. However, the ratio of deposition velocities ($ROOH/H_2O_2$), computed from normalized concentration gradients, ranged from 0.28 to 0.61 (geometric mean) at the three sites. Differences in molecular diffusivities between H_2O_2 and ROOH can only account for an estimated 16% difference in V_d. Thus, the major constituent of ROOH must also be less soluble and/or less reactive than H_2O_2, which is consistent with the characteristics of methylhydroperoxide (MHP). © 1999 Elsevier Science Ltd. All rights reserved.

Keywords: Deposition velocity; Surface resistance; Eddy diffusivity; Hydrogen peroxide; Organic peroxide

1. Introduction

Hydrogen peroxide (H_2O_2) has recently been used as an indicator species to identify the photochemical state of polluted atmospheres, i.e. whether O_3 formation in a particular region is limited by NO_x or reactive organic gases (ROG) (Sillman, 1995). The indicator species concept was derived from the desire to obtain valuable information about regional chemistry without the need for extensive measurements of the many species involved in the complex, reactive systems. Using a photochemical model, Sillman proposed that in the northeastern US a hydrogen peroxide to nitric acid ratio greater than about 0.4 indicates NO_x-limited chemistry, while $H_2O_2/HNO_3 < 0.4$ suggests a ROG-limited case. This technique provides an important check on other methods for assessing tropospheric ozone formation potential. One difficulty associated with indicator species analysis, however, is that the results depend on the dry deposition rates of many species involved, particularly NO_y, H_2O_2, and organic peroxides (ROOH) (Sillman et al., 1997).

*Corresponding author; Present address: Cooperative Research Center for Southern Hemisphere Meteorology, CSIRO, PO Box 218, West Lindfield, New South Wales, 2070 Australia. Tel.: 61 2 9413 7179; fax: 61 3 9413 7204; e-mail: office: brad.hall@tip.csiro.au.; home: vacy@ozemail.com.au.

1352-2310/99/$ – see front matter © 1999 Elsevier Science Ltd. All rights reserved.
PII: S1352-2310(98)00271-4

The uptake of pollutants by plants is responsible for a large fraction of the dry deposition flux. Trace gas uptake rates depend on the efficiency of transport to the plant surface, diffusion inside the plant cells, and subsequent degradation. The bulk resistance analogy relates the flux to a driving force (the concentration difference between the bulk air and the sink) and a combination of resistances related to aerodynamic and surface effects. For some species, such as O_3 and SO_2, the uptake is essentially controlled by a surface resistance (R_c) (Wesely and Hicks, 1977; Wesely et al., 1978). Highly soluble and reactive species such as HNO_3 and NH_3 are thought to have small or negligible surface resistances (Meyers et al., 1989; Duyzer et al., 1992), and hence their uptake is controlled mainly by turbulence.

With reliable methods for peroxide detection still relatively new, few peroxide uptake studies have been reported. Claiborn and Aneja (1993) and Ennis et al. (1990) have conducted chamber studies on conifer saplings. Their results indicate that stomata uptake of H_2O_2 to red spruce is negligible. These results, along with the fact that H_2O_2 is highly soluble and reactive, suggest efficient transport and a low surface resistance.

The bulk resistance approach has been used by Walcek (1987) and Gao et al. (1993) to predict H_2O_2 deposition velocities over the eastern US, and is generally available within most regional photochemical models. Verifying deposition models through field measurements is difficult, however. The high solubility and high reactivity of H_2O_2, along with the slow response of current sensors, make peroxide deposition measurement especially challenging. Nonetheless, some progress has been made. Deposition rates have been inferred from concentration gradients measured above wheat (Heikes et al., 1986), above a pine forest (Hall and Claiborn, 1997), and from the first-order decay of peroxide concentrations within the nocturnal boundary layer (Hastie et al., 1993). While use of the flux-gradient technique can be difficult to implement and introduces uncertainties associated with mass transfer similarity, it is often used as a starting point to measure fluxes of trace gases for which fast sensors, and hence eddy covariance techniques, are unavailable.

In this paper, a detailed description of the flux-gradient methods employed by Hall and Claiborn (1997) is presented, including an examination of difficulties and uncertainties. We present results from four field studies conducted above a mature deciduous forest, a boreal pine forest, and a managed poplar stand. We then compare the results to those obtained using a single-layer deposition model of the type often included in regional photochemical models. The measurements are used to assess the magnitude of a potential surface resistance (R_c) and various forms of the laminar leaf-layer resistance (R_b). We also report on the ratio of the deposition velocity of ROOH to that of H_2O_2.

2. Methods

2.1. Site description

Deposition velocities were measured during four summer field experiments at three different sites summarized in Table 1. Vertical gradients in peroxide concentration were measured above the forests from walk-up instrument towers. With the exception of the Boardman (BD) site, which is relatively new, all sites have been well characterized with respect to trace gas flux measurement (Meyers et al., 1989; Baldocchi et al., 1997a). The Boardman tower was located in an ideal setting for flux measurement: a homogeneous forest of uniform height, extensive fetch, and little relief.

2.2. Flux measurements

A deposition velocity (V_d, m s^{-1}) is commonly used to incorporate trace gas deposition in regional photochemical models. A deposition velocity relates the above-canopy flux (F, g m^{-2} s^{-1}) at a particular height (z, m) to the concentration (C, g m^{-3}) at that height, $F = -V_d(z)C(z)$, provided that the concentration at the sink is much less than $C(z)$. For peroxides, the assumption that $C_{sink} \ll C(z)$ is supported by the detailed transport model results of Claiborn et al. (1993). Deposition velocities

Table 1
Site description for WB (Walker Branch Watershed, Oak Ridge, TN), BR (BOREAS Old Jack Pine site, Southern Study Area, Nipawin, Sask., Canada), BD (Boise Cascade Poplar Farm, Boardman, OR). Other parameters are: d, displacement distance; h_c, canopy height; z_o, roughness length. Two heights are listed for the lower inlet at BR94 because the inlet level was raised during the experiment

Site	yr	Forest	Months	Inlet heights (m)	h_c (m)	d (m)	z_o (m)
WB	93	Mixed deciduous	Sept.	30, 39	24	$0.85h_c$	1.3
BR	94	Jack pine	May–Sept.	16.5 (17.2), 23.8	13	$0.44h_c$	2.15
WB	95	Mixed deciduous	July	34.0, 41.5	26	$0.85h_c$	1.3
BD	96	Managed poplar	Aug.–Sept.	16.4, 21.8	14	$0.80h_c$	1.1

were determined from simultaneous measurements of peroxide fluxes and concentrations.

Peroxide fluxes were determined from concentration gradients. The flux-gradient, or K-theory method, is based on the idea that under steady state, horizontally homogeneous conditions, the vertical turbulent can be expressed as the product of the vertical concentration gradient and a turbulent (eddy) diffusivity (K, $m^2\ s^{-1}$).

$$F = -K\frac{dC}{dz}. \quad (1)$$

In practice, the concentration gradient can be approximated by the differential $\Delta C/\Delta z$ by measuring concentration at two heights above the canopy, as long as the sensors are not spaced too far apart. There is, of course, a trade-off between the desire to place sensors within a nearly linear portion of the logarithmic concentration profile and the need to place sensors close enough to the source/sink so that gradients can be detected.

Concentration gradients are normally obtained by collecting integrated or sequential air samples at two or more heights above the surface. Integrated samples should be collected over a time period sufficient to encompass all time scales of mixing responsible for transport, typically 30–60 min. Sequential samples should be performed over short intervals (typically 30–60 s) to resolve the concentration profile as it evolves in time. The mean gradient is then determined over a 30–60 min period.

The application of Eq. (1) assumes a constant flux layer above the canopy. When reactive time scales are comparable to turbulence time scales, this will not be the case (see Gao et al., 1993). Reactive time scales for peroxides are on the order of hours, and are much longer than turbulence time scales over forests. Additional assumptions and approximation associated with Eq. (1) are discussed later.

2.3. Concentration measurement

Peroxide concentrations were obtained using the continuous, dual-channel, enzyme catalysed, fluorometric method (Lazrus et al., 1986). This technique is commonly used to measure tropospheric hydrogen peroxide and total organic peroxides, and has been described by Claiborn and Aneja (1991) and Hall and Claiborn (1997). This indirect method detects gas-phase peroxides by reacting peroxides in the liquid phase with *p*-hydroxyphenylacetic acid catalysed by the peroxidase enzyme. The dual-channel system detects all soluble peroxides (H_2O_2 + ROOH) in one channel, and by destroying H_2O_2 with the addition of catalase enzyme, detects primarily ROOH in the other channel. The instrument was operated in single-channel (total peroxide) mode during part of the Boardman (BD96) campaign. For the BD96 experiment, hydrogen peroxide and organic peroxide deposition velocities were derived from measurements of the total peroxide deposition velocity using the method outlined in the appendix.

Peroxide measurements were made at two heights by sequential sampling. Although switching times of 30–60 s are desired (typical for CO_2 and H_2O profile measurements (Meyers et al., 1996), rapid switching is not possible with the continuous peroxide instrument used for these studies because the e^{-1} response time is approximately 60 s. The long response time is a consequence of the lateral diffusion and mixing of the liquid within the mixing coil, tubing, and fluorescence cell. The residence time of the fluorescence cell alone was around 30 s for the conditions employed during the present experiments. Gradients were measured using sampling periods of 7–20 min at each height during WB93 and BR94 and 10 min during WB95 and BD96. Signals from the continuous peroxide analyzer were sampled at 1 Hz and stored as 20, 30, or 60 s averages.

Sequential sampling introduces error into the gradient measurement (Woodruff, 1986; Meyers, 1996). By alternately sampling continuous temperature records obtained at two heights, Woodruff (1986) estimated the sampling error, ε (%), as a function of the sampling time scale, T_s, and the turbulence time scale, τ.

$$\varepsilon = 6\left[\frac{T_s}{\tau}\right]^{0.8}. \quad (2)$$

With a turbulence time scale of 100–200 s, typical over forests (Raupach, 1989), and a sampling period of 7 min ($T_s = 14$ min), sequential sampling introduces an error of 19–33%. This error approaches 40–60% with a 15 min sampling period ($T_s = 30$ min).

2.4. Sampling bias

With any differential system, sampling bias must be considered. Materials and methods must be selected such that bias is eliminated or at least predictable. Sampling bias is particularly important for H_2O_2 because of its high solubility and reactivity. For example, for a deposition velocity of 4 $cm\ s^{-1}$, $\Delta z = 10$ m, and $K = 6\ m^2\ s^{-1}$, one would expect a ΔC of about 7%. Consequently, a bias of even a few percent can be very important.

In our initial peroxide flux experiments (WB93, BR94) (Hall et al., 1995; Hall and Claiborn, 1997) sequential sampling was performed using two short inlets coupled to a switching valve (Fig. 1a). Air was drawn through 4–5 m of 4.83 mm i.d. tubing to a three-way PFA Teflon valve and then to the peroxide analyzer, located at the base of the tower. Although the two inlet sections were of equal length and all sample lines were made of PFA Teflon, the preferred material for peroxide measurement (Lazrus et al., 1986), the buildup of dirt and other foreign

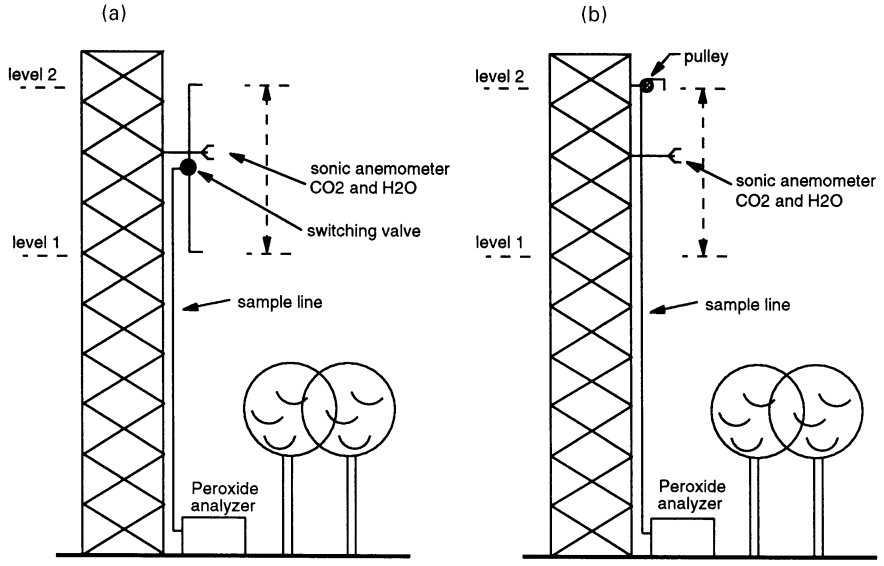

Fig. 1. Schematics of (a) gradient set-up with two inlet lines and a three-way valve, (b) gradient set-up with a single inlet line. Experiments WB93 and BR94 correspond to (a), while WB95 and BD96 correspond to (b).

matter in the inlets and valve often led to a detectable bias. This was overcome during the BR94 study through efforts to continually quantify and eliminate bias. Bias measurements were made by placing both inlet lines at the same height and sampling in the normal fashion for several hours. A bias correction factor (f_b) was computed as the average ratio $C_{\text{upper}}/C_{\text{lower}}$. The lines were then returned to their original positions and subsequent lower-level readings were multiplied by the bias correction factor.

With careful bias control (clean sample lines and frequent bias measurement), reliable flux measurements can be obtained. However, efforts to control and measure bias are difficult, time-consuming, and come at the expense of ambient sampling. Furthermore, it can be difficult to evaluate sampling bias amidst turbulent concentration fluctuations. Consequently, most bias measurements performed during BR94 were conducted at night, and there is some question as to whether these tests are representative of daytime conditions. Additionally, sudden changes in sampling bias, which might occur during periods of high aerosol loading or pollution events may go undetected. During the WB95 and BD96 studies sampling bias was minimized by the use of a single-inlet system. In this system, a single 4.83 mm i.d. PFA line was attached to a pulley and manually positioned at two heights above the canopy (Fig. 1b).

2.5. Resolving the concentration gradient

Concentration gradients have been computed in two ways. The first method involves interpolation over three consecutive measurements obtained at two levels,

$$\frac{\Delta C}{\Delta z} = \frac{C_2 - 0.5(C_1 + C_3)}{\Delta z} \tag{3}$$

where C_2 (ppb) is the average concentration at the upper level, and C_1 and C_3 (ppb) are the average concentrations at the lower level observed immediately before and after C_2. An advantage of this method is that atmospheric or instrumental changes that occur on the order of the time required to resolve the gradient can be examined. A large fluctuation in concentration during any one of the three periods might indicate a disruption of the pseudo-steady-state condition required for the application of the flux-gradient method. Individual gradient measurements can be evaluated by looking at the statistics associated with each C_i measurement. The various sources of concentration fluctuations can lead to a highly variable deposition record in which individual measurements carry little significance. The WB93 and BR94 data were reduced by rejecting any gradient measurement period (consisting of three samples) for which the standard deviation of the mean of any one sample exceeded 5% of its corresponding mean concentration. This procedure results in the rejection of many extreme V_d values without significantly affecting the overall results.

In the second method, the gradient is computed from a moving average fit to the concentration record at each level,

$$\frac{\Delta C}{\Delta z} = \frac{C'_{\text{upper}} - C'_{\text{lower}}}{\Delta z} \tag{4}$$

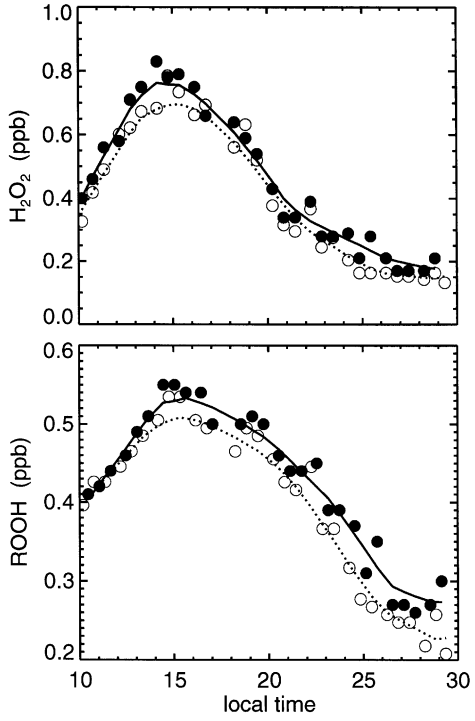

Fig. 2. A sample of data collected during the BR94 experiment (day 205–206). Each plot shows concentration (ppb) at the lower inlet level (open symbols and dashed line) and at the upper inlet level (filled symbols and solid line). Lines represent moving average fits to the data.

where C'_{upper} and C'_{lower} are the smooth-fit concentrations at a particular time. While a number of curve fitting strategies could be employed, the numerous time scales of variation make parametric methods (such as polynomial fitting) difficult and case-specific. Moving-average smoothing seems to work well, although the choice of filter width can be subjective. Computing ΔC from moving averages helps to smooth out the effects of instrument variations and fluctuations in concentration and also reduces the number of extreme V_d. Examples of smoothed concentration records (1.5 h moving average) from the BR94 experiment are shown in Fig. 2. In this example, a concentration difference between upper and lower sampling heights was clearly resolved throughout most of the period.

Deposition velocities of H_2O_2 computed using both methods are shown in Fig. 3 for a 5-day period during BR94. Both methods exhibit about the same amount of variability and produce similar results. The smoothing method fails when the data record is frequently interrupted or contains only a few samples. The smoothing method was applied to the WB95 and BD96 data, while the interpolation method was applied to WB93 and BR94 data.

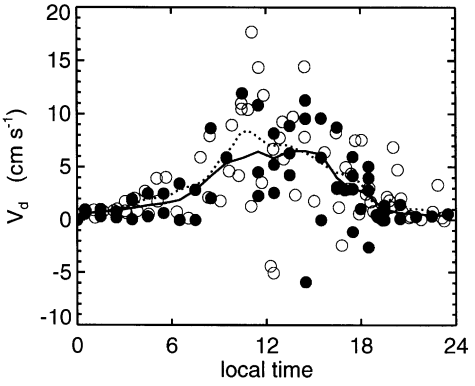

Fig. 3. H_2O_2 deposition velocities (cm s^{-1}) determined using the interpolation method (open symbols and dashed line) and the smooth fit method (filled symbols and solid line) during the BR94 experiment (days 205–209).

2.6. Eddy diffusivities

Since eddy diffusivities for many trace gases are not readily available, it is usually assumed that trace gases are transported in a manner similar to that of other scalars, such as heat, water vapor, or carbon dioxide. Eddy diffusivities can be estimated from similarity relationships (see for example Kaimal and Finnigan, 1994) or measured directly by simultaneously measuring the flux and concentration gradient of a particular species:

$$K_i = -\frac{F_i}{\Delta C_i/\Delta z}. \tag{5}$$

When direct measurements of K for one species are applied to another species, it is known as the modified Bowen ratio method. This approach circumvents the problems of K enhancement associated with the application of Monin–Obukhov similarity theory over rough forests (Raupach, 1979; Cellier and Brunet, 1992).

For a particular eddy diffusivity to be applicable to another species, the distribution of sources and sinks should be similar. As a first approximation, one might think that water vapor or CO_2 would be good choices because they are emitted/absorbed by leaves during transpiration/photosynthesis, just as peroxides are deposited to leaf and plant tissue. Since soil may also be a significant source for CO_2, however, it is generally felt that K_c (CO_2) should not be applied to peroxide deposition because the distribution of CO_2 sources/sinks does not coincide with those of peroxide.

Several eddy diffusivities were determined simultaneously when possible. Eddy diffusivities for heat (K_h), water vapor (K_q), and CO_2 (K_c) were measured during BR94 and K_q and K_c were measured during WB95. The eddy diffusivity for heat was also estimated during each experiment using standard Monin–Obukhov similarity

theory (Kaimal and Finnigan, 1994) and is hereafter referred to as $K_{h(MO)}$. Water vapor and CO_2 gradients were measured with a closed-path infra-red gas analyzer (IRGA) (model LI-6262, LICOR, Lincoln, Nebraska). Air was sampled sequentially from four levels on the towers (two above the canopy and two within the canopy). Air samples were analyzed for 20 s and switched among the four levels every 30 s. The LI-6262 was zeroed and spanned once per day. The above-canopy inlet locations corresponded to those of the peroxide gradient system. Temperature gradients were measured during BR94 using high-quality thermocouples (Frenzen and Vogel, 1995). Water and CO_2 fluxes were measured using a 3-D sonic anemometer (model SWS-211/3K, Applied Technology Inc., Boulder, Colorado) and an open-path IRGA (Auble and Meyers, 1992) while sensible heat fluxes were determined from temperatures reported by the sonic anemometer (see Baldocchi et al., 1997a, b).

Deposition velocities were determined using measured values of K_h or K_q whenever possible. $K_{h(Mo)}$ was used to fill in for missing values of K_h or K_q (24 out of 377 observations during BR94, and 15 out of 105 observations during WB95). $K_{h(Mo)}$ was used exclusively during WB93 and BD96 for lack of ancillary K measurements.

As previously mentioned, there are problems associated with the application of Monin–Obukhov theory over tall forests, particularly within the roughness sublayer. Eddy diffusivities do not often agree with their Monin–Obukhov values. However, $K_{h(Mo)}$ was a surprisingly reasonable substitute for K_h and K_q during BR94 and WB95 (to be shown later). This may be because the inlets were known to be located above the roughness sub-layer during the BR94 and WB95 experiments. The location of the lower-level inlet with respect to the roughness sub-layer is not well known for the BD96 experiment. If we take the roughness sub-layer depth as 3–4 times the mean distance between canopy elements (Cellier and Brunet, 1992), the position of the lower level inlet at BD96 was probably marginal.

We anticipated that K_h and K_q would be most applicable to peroxides because of the similarity of sources and sinks. However, at high solar elevation angles a significant fraction of the net radiation reached the forest floor at the BR94 site (Baldocchi et al., 1997b). This resulted in significant latent and sensible heat sources at the forest floor. A surface source for a particular scalar would reduce the effective displacement distance and lead to an enhancement of its eddy diffusivity. Hence, deposition velocities may be overestimated at this site. This assumes, however, that peroxides are lost primarily to leaf tissue in the upper canopy. We cannot rule out the possibility of peroxide losses to woody tissue and the forest floor, which would mean that measured K_h and K_q could very well be appropriate at this site. Ultimately, independent peroxide flux measurements are required to fully address the eddy diffusivity question.

The usefulness of a particular K also depends on how well it can be measured or approximated. During the BR94 experiment, water gradients were small and difficult to measure due to low latent heat fluxes (Baldocchi et al., 1997b). Consequently, measurements of K_q did not prove useful due to extreme variability.

A re-examination of the temperature gradients obtained during BR94 revealed a slight bias between the two sensors employed in this study. A bias of $0.05 \pm 0.01^{\circ}C$ (K_h underestimated) was identified by plotting ΔT against the sensible heat flux. With a $0.05^{\circ}C$ correction applied to the ΔT measurements, midday K_h values are increased by an average of 25%. Therefore, midday deposition velocities reported here for BR94 are, on average, 25% larger than those reported by Hall and Claiborn (1997). A comparison of eddy diffusivities obtained during BR94, both before and after the bias correction, is shown in Fig. 4. The bias correction has brought midday K_h values into surprisingly good agreement with $K_{h(MO)}$. Similar plots of K_q, K_c, and $K_{h(MO)}$ for WB95 are shown in Fig. 5. On average, K_c, K_q, and $K_{h(MO)}$ showed relatively good agreement at the WB site as well, indicating that $K_{h(MO)}$ is a reasonable substitute for K_q at this site.

In summary, all deposition velocities were computed using either K_h, K_q, or $K_{h(MO)}$ depending on availability. For the WB site, the choice of eddy diffusivity has a 25% effect on daytime fluxes. The data reported here for WB95 have been computed using K_q, which were, on average, less than K_c and $K_{h(MO)}$. The influence of our choice of K is unknown at the BR94 site because measurements of K_q and K_c were not successful due to small CO_2 and water gradients. Little information is available concerning the quality of the K estimated at the

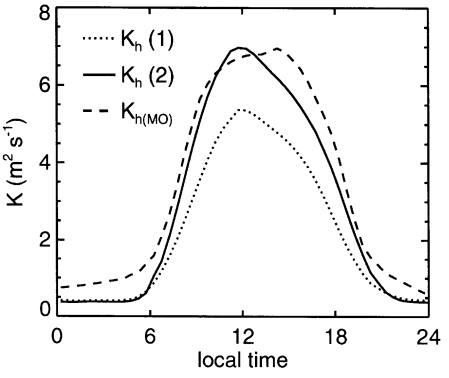

Fig. 4. Comparison of eddy diffusivities ($m^2\ s^{-1}$) from the BR94 experiment ($K_h(1)$ is K_h without the temperature gradient correction, $K_h(2)$ is K_h with the temperature correction, see text). Curves represent four hour moving averages of K (approximately 3000 half-hour observations). The standard deviations of residuals associated with the smooth fits are 2.2, 2.3, and 1.6 $m^2\ s^{-1}$ for $K_h(1)$, K_h (2), and $K_{h(MO)}$, respectively.

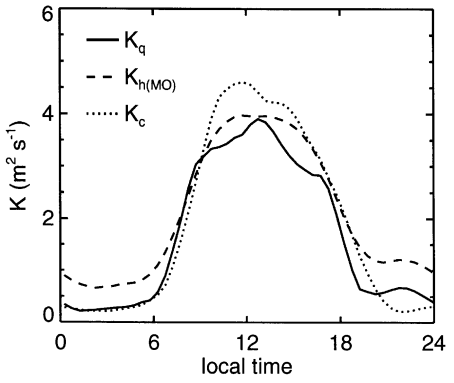

Fig. 5. Comparison of eddy diffusivities from the WB95 experiment (thin solid curves represent four hour moving averages of K (approximately 400 half-hour observations). The standard deviations of residuals associated with the smooth fits are 1.5, 1.6, and 0.6 $m^2 s^{-1}$ for K_c, K_q, and $K_{h(MO)}$, respectively.

BD96 site. Simultaneous measurements of isoprene flux by relaxed eddy accumulation and flux-gradient methods (Hall et al., 1997) have shown that $K_{h(MO)}$ may underestimate K by roughly 30% at this site, but these results are difficult to interpret because many of these experiments were conducted under convective conditions with light and variable winds. Peroxide deposition velocities reported here probably represent an upper limit at the BR94 site and may be somewhat underestimated at the BD96 site.

2.7. Summary of uncertainties

The precision (standard deviation of the mean) based on the continuous sampling of a slowly varying H_2O_2 concentration is roughly 0.5–1.5%. In a turbulent atmosphere, the precision associated with a 7–20 min sampling period can range from 1–10%. The uncertainty in measured K is about 40%. The combination of uncertainties associated with K, sequential sampling, bias, and concentration measurement results in uncertainties of approximately 40–100% for individual deposition velocity measurements, even under the best of conditions. Accordingly, large data sets, careful data screening, and composite averaging of the resulting V_d are required.

3. Results and discussion

3.1. Diurnal variations of V_d

If peroxide deposition is controlled mainly by turbulence V_d should exhibit a diurnal variation. The diurnal variation of H_2O_2 V_d at the BR94 site can be seen in Fig. 3. Diurnal trends of H_2O_2 V_d were also observed during WB93 and BR94 for ROOH (not shown). Diurnal trends were not obvious during WB95 and BD96, most likely because few nighttime samples were obtained.

Another important difference between the WB93-BR94 and WB95-BD96 relates to the gradient sampling method (switching valve versus single inlet line). Although new sample tubing and a new sample valve were used during WB93, rigorous bias checks were not performed in the field; thus, we cannot rule out the possibility that the WB93 data are biased. Line-loss measurements performed in the laboratory under ideal conditions (constant temperature, low relative humidity) revealed losses of approximately 5% (as H_2O_2) for the entire sampling system employed during WB93. Line losses were measured by sampling a non-varying H_2O_2 source through the same tubing and valves system used in the field and comparing the signal with that obtained through a minimal about of tubing. While losses in the valve and inlet sections were small and presumed equal, a bias of only a few percent would have significantly affected the results. The BR94 data deserve greater confidence because of the careful bias control efforts employed and the large data set obtained.

3.2. Modeling H_2O_2 V_d

Here we consider the application of modeling peroxide deposition within the framework of a regional-scale photochemical model. Bulk resistance methods are computationally attractive for such applications. While problems may arise under some conditions, low LAI for example, the benefits gained by the fine detail of a multilayer model might not be realized given the uncertainties associated with estimating surface characteristics on regional scales. Therefore, bulk resistance methods need to be assessed in the context of how they are likely to be applied.

A common form for the bulk resistance model (Wesely and Hicks, 1977) is given by,

$$V_d^{-1} = R_a + R_b + R_c = \frac{1}{ku_*}\left[\ln\frac{z-d}{z_0} - \Psi\left(\frac{z}{L}\right)\right] + \frac{2}{ku_*}\left[\frac{Sc}{\mathrm{Pr}}\right]^p + R_c \quad (6)$$

where R_a is the aerodynamic resistance, R_b is the quasi-laminar leaf-layer resistance, and R_c is the surface resistance. The first term in the expanded form corresponds to R_a, where k is the von Karman constant (0.4), u_* (m s^{-1}) is the friction velocity, z_0 (m) is the surface roughness, d (m) is the displacement distance, Ψ is a stability correction factor and L (m) is the Monin–Obukhov length. The second term corresponds to R_b, where Sc is the Schmidt number ($\mu/\rho D_i$), μ (kg $m^{-1} s^{-1}$) is the viscosity of air,

ρ (kg m^{-3}) is the air density, and D_i (m^2 s^{-1}) is the molecular diffusivity of the trace species in air, Pr is the Prandtl number ($\mu/\rho\alpha$), α (m^2 s^{-1}) is the thermal diffusivity of air, and p is normally 2/3.

For the particular case where $R_c = 0$, V_d should, to a first approximation, be proportional to u_*,

$$V_d = ku_* \left[\ln \frac{z-d}{z_o} - \Psi\left(\frac{z}{L}\right) + 2\left[\frac{\alpha}{D_i}\right]^p \right]^{-1}. \quad (7)$$

Fig. 6 shows measured V_d for H_2O_2, a best-fit line through the data, and V_d predicted using Eq. (7). Although there is substantial scatter in the data, the general dependence of V_d on u_* can be seen.

While the form of R_a in Eq. (6) is commonly used, there remains some question regarding the identity of R_b. For trace gases that exhibit a significant surface resistance, such as O_3 and SO_2, the exact form of R_b is relatively unimportant because R_c tends to dominate. For H_2O_2, however, it is worth taking a closer look at R_b.

The dependence of R_b on Schmidt and Prandtl numbers shown in Eqs. (6) and (7) was derived from an analogy with heat transfer to flat plates (Pearman et al., 1972). Uncertainties in the boundary layer resistance arise when one considers various shapes and arrangements of the roughness elements, the sheltering effect of bunched leaves, and deposition to non-leaf elements. In fact, there is some question as to the validity of the single-layer bulk transfer approach in which R_b and R_c appear as separate entities (Bache, 1986). Nevertheless, single-layer models offer a practical solution to trace gas transport if they can be shown to provide reasonable results in most cases.

The resistance R_b can also be expressed as $B^{-1}u_*^{-1}$, where B^{-1} is the Stanton number (a non-dimensional bulk parameter introduced by Owen and Thomson, 1963). The Stanton number is often combined with the Von Karman constant and expressed as kB^{-1}. In Eq. (7) kB^{-1} takes the form $2(\alpha/D_i)^p$.

$$V_d = ku_* \left[\ln \frac{z-d}{z_0} - \Psi + kB^{-1} \right]^{-1}. \quad (8)$$

In general, kB^{-1} varies with surface type and appears to be either nearly constant, or a strong function of the roughness Reynolds number ($Re_* = \rho u_* z_0/\mu$) (Garratt and Hicks, 1973). With $kB^{-1} = 2(Sc/Pr)^{2/3}$, kB^{-1} is equal to 2.5 for H_2O_2. Brutsaert (1975) reported the relation

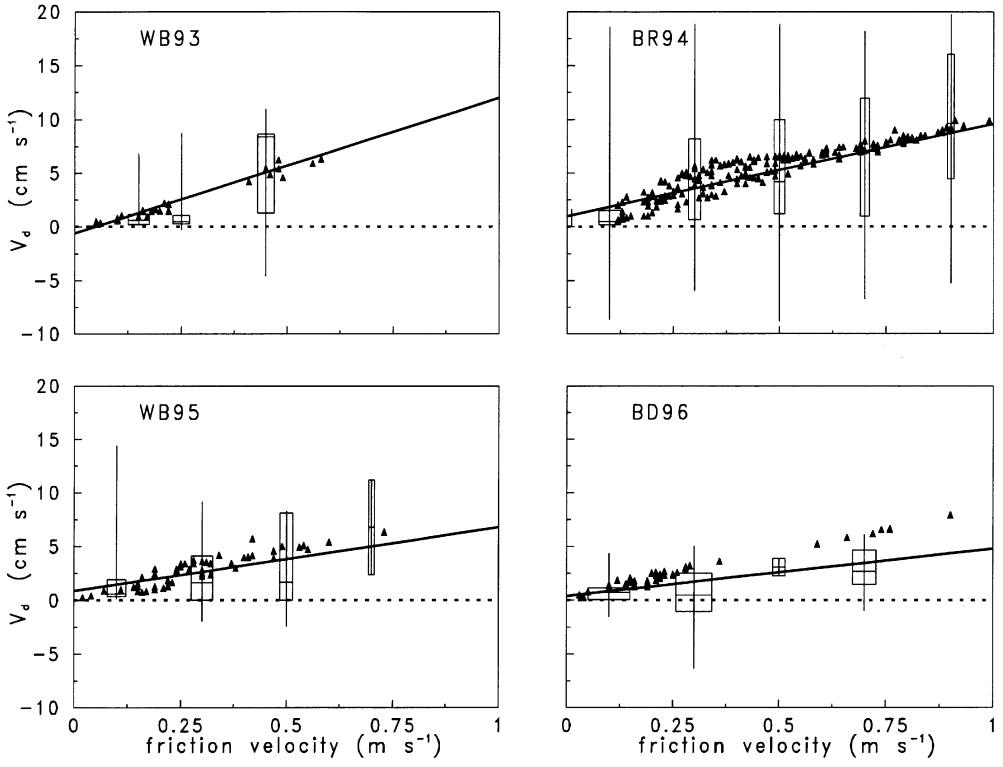

Fig. 6. Measured (box plots) and predicted (filled triangles) deposition velocities of H_2O_2 (cm s^{-1}) at each site as a function of u_* (m s^{-1}). Box plots show the minimum, maximum, 25th, 50th, and 75th percentiles. The solid lines are least squares fits to the data. The $V_d = 0$ line (dashed line) is included for reference.

$kB^{-1} = 2.92Re_*^{0.25}Sc^{0.5}$–2.0 based on wind tunnel studies. This equation results in much higher values of kB^{-1} at high Re_* typical over forests ($Re_* > 10^3$). For example, for the BR94 pine forest with $u_* = 0.5\ \mathrm{m\,s^{-1}}$ and $z_o = 2.15$ m, Re_* is 7.2×10^4 and kB^{-1} becomes 46. The H_2O_2 V_d predicted by Eq. (8) under neutral conditions is $0.5\ \mathrm{cm\,s^{-1}}$. Using the best-fit line shown in Fig. 6 as a guide, measurements would suggest a V_d of about $5\ \mathrm{cm\,s^{-1}}$. The same situation applied to the BD96 site yields a predicted V_d of $0.5\ \mathrm{cm\,s^{-1}}$ and a measured V_d of about $2.5\ \mathrm{cm\,s^{-1}}$. Clearly, this form for kB^{-1} does not apply to the forests studied in the present experiments.

Forms for kB^{-1} that do not depend on Re_* have also been suggested. Jensen and Hummelshoj (1995, 1997) showed that kB^{-1} could be related to the size of the individual leaf/needle elements and LAI. Using their relationship derived from measurements of water vapor flux over a spruce forest we estimate kB^{-1} to be around 6 for BR94 at $u_* = 0.5$. The corresponding predicted V_d of $2.5\ \mathrm{cm\,s^{-1}}$ is still substantially less than what was observed. Thom (1972) showed that the transport of heat and water vapor to/from vegetation should conform to $kB^{-1} = 2.5u_*^{1/3}$ (with u_* in $\mathrm{m\,s^{-1}}$). Under the same conditions as before for the BR94 site, kB^{-1} would be 2.1 and the predicted V_d would be $5.1\ \mathrm{cm\,s^{-1}}$. We conclude that a kB^{-1} in the range 2–3, as predicted from $kB^{-1} = 2(Sc/Pr)^{2/3}$ or $kB^{-1} = 2.5u_*^{1/3}$, is appropriate for H_2O_2 transport the forest canopies studied here.

Deposition velocities predicted using Eq. (8) with $kB^{-1} = 2.5$ and $R_c = 0$ are shown in Fig. 6. For comparison, predicted V_d would be about 15% larger if the expression $kB^{-1} = 2.5u_*^{1/3}$ were used. The diabatic stability correction factor, ψ, was computed according to Wesely and Hicks (1977) and is valid for $-1 < z/L < 1$. Roughness lengths and displacement distances were determined by fitting the logarithmic wind speed equation (Stull, 1988) to wind speed observed above the canopy under neutral conditions. Molecular diffusivities of 0.156 and $0.108\ \mathrm{cm^2\,s^{-1}}$ were used for H_2O_2 and ROOH, respectively. The diffusivity for H_2O_2 was obtained by scaling the value reported by McMurtrie and Keyes (1948) ($0.188\ \mathrm{cm^2\,s^{-1}}$ at 60°C) to 25°C assuming a $T^{1.75}$ temperature dependence. The diffusivity of ROOH at 25°C was obtained by multiplying $D_{H_2O_2}$ by the ratio of diffusivities ($D_{ROOH}/D_{H_2O_2} = 0.69$) predicted by a variation of the Gilliland method (Fuller and Giddings, 1965), assuming that methylhydroperoxide (MHP) was the dominant organic peroxide present. These diffusivities correspond to kB^{-1} values of 2.5 and 3.2 for H_2O_2 and ROOH, respectively.

Predicted V_d generally show good agreement with the measurements except for the BD96 site. As previously mentioned, $K_{h(MO)}$ employed at this site may have been underestimated by about 30%. A 30% increase in $K_{h(MO)}$ would result in better agreement between the measured and predicted V_d at the BD96 site. The significant scatter in the data observed at all sites may expose the difficulties associated with using the flux-gradient method to measure peroxide deposition velocities above tall forests, particularly under convective conditions. It is clear that light winds and convective conditions are not conducive to the methods of sequential sampling employed during these studies. We must also keep in mind that the single-layer model is based upon the assumption that the concentration of the depositing species is constant with height in the canopy. For peroxides this is clearly not the case. A significant draw down of peroxide concentration within the canopy was observed at all sites. Baldocchi (1992) has shown that the assumption of height-invariant concentration leads to an overestimate of V_d compared to a Lagrangian random-walk model. In addition, one would not expect the single-layer model to perform equally well for different leaf area indices. Multi-layer models suggest that V_d scales with leaf area index (LAI) for low LAI values and saturates at high LAI (Meyers et al., 1989; Baldocchi, 1992). Nevertheless, the best-fit lines in Fig. 6 are remarkably similar to the predicted V_d.

We now compare our results with those predicted by the single-layer model by computing R_c (using Eq. (6)) and testing the hypothesis that $R_c = 0$. Because R_c has a lower bound at zero, by definition, V_d less than zero were excluded from the calculation of R_c. A 2σ filter was also applied to remove extreme values that arise from V_d close to zero. Geometric mean values of R_c were determined to be $4\ \mathrm{s\,m^{-1}}$ during BR96, $6\ \mathrm{m\,s^{-1}}$ during WB95, and $13\ \mathrm{s\,m^{-1}}$ during WB93. These values are not significantly different from zero at the 95% confidence level (Rinaman, 1993). A 30% decrease in K (eddy diffusivity) would result in a small but non-zero surface resistance for H_2O_2 at all sites.

Fig. 7 shows measured ROOH V_d along with model predictions using $R_c = 0$. The lower diffusivity of ROOH accounts for a 16% reduction in V_d relative to that of H_2O_2. This is not enough to explain the observed differences in V_d between H_2O_2 and ROOH. Clearly, the assumption that $R_c = 0$ is incorrect for ROOH. It is difficult to test the significance of R_c (ROOH), however, because uncertainties associated with the ROOH V_d measurements are higher than those associated with H_2O_2, due to lower concentrations of ROOH relative to H_2O_2.

The geometric mean R_c for ROOH was determined to be around $15\ \mathrm{s\,m^{-1}}$ during BR94 and 20–40 $\mathrm{s\,m^{-1}}$ during WB93 and WB95. The observed R_c for ROOH are significantly different from zero for all sites. This conclusion still holds if K is increased by 30%. The observed R_c are similar in magnitude to minimum R_c typically associated with SO_2 and O_3 dry deposition (Wesely and Hicks, 1977; Padro, 1996).

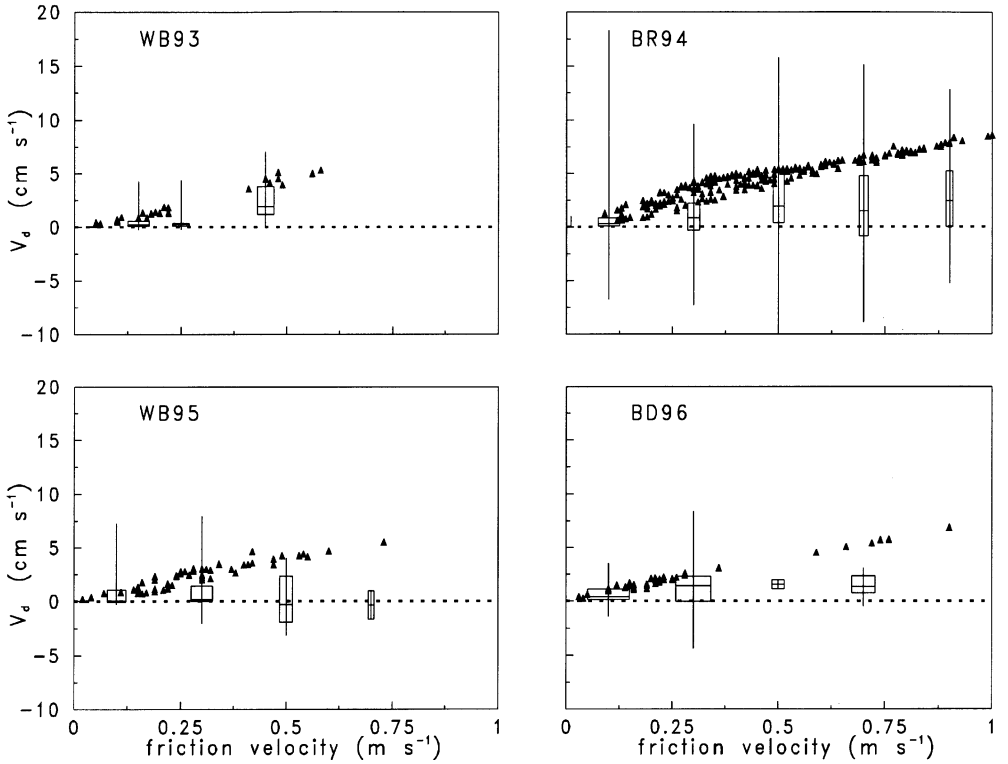

Fig. 7. Measured (box plots) and predicted (filled triangles) deposition velocities of ROOH (cm s^{-1}) at each site as a function of u_* (m s^{-1}). Predicted V_d were computed using $R_c = 0$. The $V_d = 0$ line (dashed line) is included for reference.

3.3. Comparing V_d for H_2O_2 and ROOH

An alternate method for specifying V_d(ROOH) in regional photochemical models would be to specify V_d(ROOH) as a fraction of $V_d(H_2O_2)$. The ratio of V_d(ROOH) to $V_d(H_2O_2)$ can be determined directly from the ratio of normalized concentration gradients, and is therefore devoid of errors associated with estimating the eddy diffusivity. The results from the four studies described here are summarized in Table 2. It is interesting that the mean ratio of deposition velocities is fairly similar (within experimental uncertainties) for all cases. This may indicate that a particular organic peroxide is present at all sites. Measurements of organic peroxides made during the BR94 campaign revealed that methyl hydroperoxide (MHP) was the dominant peroxide present (A. Jackson, personal communication). MHP is much less soluble than H_2O_2, implying a lower deposition velocity. MHP is expected to be the primary organic peroxide in the remote troposphere (Logan et al., 1981). Ratios much less than one are consistent with the hypothesis that MHP, rather than the highly soluble hydoxymethyl hydoperoxide (HMHP), is responsible for a substantial portion of the organic peroxide signal observed during the present experiments.

Table 2
Ratio of V_d(ROOH) to $V_d(H_2O_2)$ determined at four sites

Exp.	N	Mean	Standard error	Median	Geometric mean
WB93	27	0.53	0.13	0.47	0.49
BR94	377	0.39	0.06	0.38	0.39
WB95	47	0.22	0.07	0.17	0.28
BD96	28	0.38	0.21	0.41	0.61

The large uncertainty associated with the Boardman data is due to the low (<1 ppb) peroxide concentrations observed during that study. Organic peroxide levels were often near the detection limit. The oxidation of isoprene, emitted by poplar, is known to generate peroxy radicals which should lead to the production of organic peroxides (Kleinman, 1986; Horie et al., 1994). However, the area surrounding the poplar farm consists of sage brush and farmland (2 km upwind). Because the concentration of peroxides reflects the time history of the air mass as well as local production and loss, peroxide by-products of an isoprene source may only be significant downwind of the site.

4. Conclusions

The dry deposition velocities of H_2O_2 and ROOH were measured over three forest types during four field campaigns. Measured H_2O_2 deposition velocities show a general dependence on u_* at each site. This suggests that a single-layer resistance-based approach can be used to incorporate peroxide V_d in regional photochemical models. For small surface resistances, correct specification of the viscous layer resistance, R_b, becomes important. Assuming a negligible surface resistance, the measured H_2O_2 V_d are consistent with the most common form for R_b, based on Schmidt and Prandtl numbers.

By comparing measured V_d to the bulk resistance model, we found that the surface resistance associated with H_2O_2 deposition is small (less than $5\,s\,m^{-1}$) when kB^{-1} is taken as 2.5. Deposition velocities of ROOH were lower than those of H_2O_2. The difference in molecular diffusivities accounts for a 16% difference between V_d(ROOH) and $V_d(H_2O_2)$. This is not enough to explain the observed differences in V_d, and suggests a non-zero surface resistance. Geometric mean values of R_c for ROOH ranged from about $15\,s\,m^{-1}$ over the pine forest to 20–$40\,s\,m^{-1}$ over the deciduous forests.

Although the uncertainties in V_d measurement and modeling do not permit a detailed assessment of R_c for organic peroxides, the ratio of V_d(ROOH) to $V_d(H_2O_2)$ can be determined. This useful result is independent of estimates of eddy diffusivity, and is recommended for use in regional photochemical models. The ratios of deposition velocities (geometric mean) were consistently less than 1.0, ranging from 0.29 to 0.61. The fact that V_d(ROOH) was less than $V_d(H_2O_2)$ indicates that the dominant organic peroxide observed was less soluble and/or less reactive than H_2O_2, which is consistent with the characteristics of MHP, rather than hydroxymethyl hydroperoxide.

Acknowledgements

We thank Bryan Clode (Washington State University) for his assistance in the laboratory and during the BD96 experiment. We also thank Boise Cascade Corporation for providing access to their managed poplar plantation. Temperature gradients for BR94 were kindly provided by Chris Vogel of the National Oceanic and Atmospheric Administration. Funding was provided by the National Science Foundation under grants ATM-9221312 and ATM 9508417, the NOAA Global Change Program, and by the U.S. Environmental Protection Agency through cooperative agreement (CR822907-01).

Appendix

Due to time constraints, some of the Boardman data were obtained by measuring only total peroxide concentration. It is possible to compute deposition velocities for both H_2O_2 and ROOH when only the total deposition velocity V_d(total) is measured provided that the ratio of deposition velocities, (f_v), and the fraction of total peroxide present as H_2O_2, (f_c), are known,

$$V_d(H_2O_2) = \frac{V_d(\text{total})}{f_v + f_c + f_v f_c} \tag{A.1}$$

where $f_v = V_d(\text{ROOH})/V_d(H_2O_2)$ and $f_c = C_{H_2O_2}/C_{\text{total}}$. The ratio f_v is obtained from the ratio of normalized concentration gradients. The deposition velocity of organic peroxides can then be computed from f_v and $V_d(H_2O_2)$. Normally, the concentration ratio (f_c) is fairly constant during midday periods and is easily measured. The concentration ratio will vary diurnally, however, as H_2O_2 is depleted more rapidly than ROOH within the nocturnal boundary layer. Midday peroxide V_d measured at the BD96 site were evaluated using an f_v of 0.5 ± 0.2 and an f_c of 0.59 ± 0.02. The large uncertainty associated with f_v is attributed to the low concentrations of peroxide observed at the Boardman site and the fact that most V_d observations occurred during periods of light wind. One third of the Boardman data were reduced using Eq. (A.1).

References

Auble, D.L., Meyers, T.P., 1992. An open path, fast response infrared absorption gas analyzer for H_2O and CO_2. Boundary Layer Meteorology 59, 243–256.

Bache, D.H., 1986. On the theory of gaseous transport to plant canopies. Atmospheric Environment 20 (7), 1379–1388.

Baldocchi, D.D., Vogel, C.A., Hall, B.D., 1997a. Seasonal variation of carbon dioxide exchange rates above and below a boreal jack pine forest. Agriculture and Forest Meteorology 83, 147–170.

Baldocchi, D.D., Vogel, C.A., Hall, B.D., 1997b. Seasonal variation of energy and water vapor exchange rates above and below a boreal jack pine forest canopy. Journal of Geophysical Research 102 (24), 28939–28952.

Baldocchi, D.D., 1992. On estimating HNO_3 deposition to a deciduous forest with a Lagrangian random-walk model. In: Schwartz, S.E., Slinn, W.G.N. (Eds.), Precipitation Scavenging and Atmosphere-Surface Exchange. Hemisphere Publishing, Washington DC, pp. 1081–1093.

Brutsaert, W., 1975. The roughness length for water vapor, sensible heat, and other scalars. Journal of Atmospheric Science 32, 2028–2031.

Cellier, P., Brunet, Y., 1992. Flux-gradient relationships above tall plant canopies. Agriculture Forest Metorology 58, 93–117.

Claiborn, C.S., Aneja, V.P., 1993. Transport and fate of reactive trace gases in red spruce needles, 1. Uptake of gaseous hydrogen peroxide as measured in controlled chamber flux experiments. Environment Science and Technology 27, 2585–2592.

Claiborn, C.S., Carbonell, R.G., Aneja, V.P., 1993. Transport and fate of reactive trace gases in red spruce needles, 2. Interpretation of flux experiments using gas transport theory. Environment Science and Technology 27, 2593–2605.

Claiborn, C.S., Aneja, V.P., 1991. Measurements of atmospheric hydrogen peroxide in the gas phase and in cloud water at Mt. Mitchell, North Carolina. Journal of Geophysical Research 96, 18771–18787.

Duyzer, J.H., Verhagen, H.L.M., Weststrate, J.H., Bosveld , F.C., 1992. Measurement of the dry deposition flux of NH_3 on to a coniferous forest. Environmental Pollution 75, 3–13.

Ennis, C.A., Lazrus, A.L., Zimmerman, P.R., Monson, R.K., 1990. Flux determinations and physiological response in the exposure of red spruce to gaseous hydrogen peroxide, ozone, and sulfur dioxide. Tellus 42B, 2.

Frenzen, P., Vogel, C.A., 1995. TKE budget measurements in the surface layer above a forest. In: Eleventh Symposium on Boundary Layers and Turbulence, American Meteorological Society, Charlotte, North Carolina, March 27–31.

Fuller, E.N., Giddings, J.C., 1965. A comparison of methods for predicting gaseous diffusion coefficients. Journal of Gas Chromatography 3, 222–227.

Gao, W., Wesley, M.L., Doskey, P.V., 1993. Numerical modeling of the turbulent diffusion and chemistry of NO_x, O_3, isoprene, and other reactive trace gases in and above a forest canopy. Journal of Geophysical Research 98, 18339–18353.

Garratt, J.R., Hicks, B.B., 1973. Momentum, heat, and water transfer to and from natural and artificial surfaces. Quarternary Journal of Royal Metorological Society 99, 680–687.

Hall, B.D., Claiborn, C.S., 1997. Measurements of the dry deposition velocity of peroxides to a Canadian boreal forest. Journal of Geophysical Research 102 (24), 29343–29354.

Hall, B.D., Claiborn, C.S., Howard, H., Baldocchi, D.D., 1995. Deposition of gas phase peroxides: measurements in a deciduous forest. In: Watson, J.G., Chow, J.C., Solomon, P.A. (Eds.), Transactions on Regional Photochemical Measurement and Modeling Studies. Technical Report, TR-24, Air and Waste Management Association Pittsburgh, Penn.

Hall, B.D., Lamb, B., Claiborn, C., Westberg, H., Baldocchi, D., Guenther, A., Harley, P., Klinger, L., Zimmerman, P., 1997. Isoprene flux measurements, modeling, and associated uncertainties at the canopy scale. Journal of Applied Meteorology, submitted.

Heikes, B.G., Kok, G.L., Lazrus, A.L., Walega, J.G., 1986. Measured surface flux of H_2O_2 vapor to wheat. EOS Transactions of the American Geophysical Union 67, 885.

Hastie, D.R., Shepson, P.B., Sharma, S., Schiff, H.I., 1993. The influence of the nocturnal boundary layer on secondary trace species in the atmosphere at Dorest, Ontario. Atmospheric Environment 27A, 533–541.

Horie, O., Need, P., Limbach, S., Moortgat, G., 1994. Formation of formic acid and organic peroxides in ozonolysis of ethene with added water vapor. Geophysical Research Letters 21, 1523–1526.

Jensen, M.O., Hummelshoj, P., 1995. Derivation of canopy resistance for water vapor fluxes over a spruce forest, using a new technique for the viscous sublayer resistance, Agriculture Forest Meteorology 73, 339–352.

Jensen, M.O., Hummelshoj, P., 1997. Erratum to derivation of canopy resistance for water vapor fluxes over a spruce forest, using a new technique for the viscous sublayer resistance. Agiculture Forest Meteorology 85, 289.

Kaimal, J.C., Finnigan, 1994. Atmospheric Boundary Layer Flows: Their Structure and Measurement. Oxford University Press, New York, N.Y., pp. 15–19.

Kleinman, L.I., 1986. Photochemical formation of peroxides in the boundary layer. Journal of Geophysical Research 91, 10889–10904.

Lazrus, A.L., Kok, G.L., Lind, J.A., Girtlin, S.N., Heikes, B.G., Shetter, R.E., 1986. Automated fluorometric method for hydrogen peroxide in air. Analalytical Chemistry 58, 594–597.

Logan, J.A., Prather, M.J., Wofsy, S.C., McElroy, M.B., 1981. Tropospheric chemistry. Global perspective. Journal of Geophysical Research, 86, 7210–7254.

McMurtrie, R.L., Hayes, F.G., 1948. A measurement of the diffusion coefficient of hydrogen peroxide vapor into air. Journal of American Chemical Society 70 (3), 3755–3758.

Meyers, T.P., Hall, M.E., Lindberg, S.E., Kim, K., 1996. Use of the modified Bowen-ration technique to measure fluxes of trace gases. Atmospheric Environment 30 (19), 3321–3329.

Meyers, T.P., Huebert, B.J., Hicks, B.B., 1989. HNO_3 deposition to a deciduous forest. Boundary Layer Meteorology 49, 395–410.

Owen, P.R., Thomson W.R., 1963. Heat transfer across rough surfaces. Journal of Fluid Mechanics 15, 321–334.

Padro, J., 1996. Summary of ozone dry deposition velocity measurements and model estimates over vineyard, cotton, grass, and deciduous forest in summer. Atmospheric Environment 30 (13), 2363–2369.

Pearman, G.I., Weaver, H.L., Tanner, C.B., 1972. Boundary layer heat transfer coefficients under field conditions. Agriculture Forest Meteorology 10, 83–92.

Raupach, M.R., 1979. Anomolies in flux-gradient relationships over forests. Boundary Layer Meteorology 16, 467–486.

Raupach, M.R., 1989. Stand overstory processes. Phil. Transactions Royal Society of London 324, 175–190.

Rinaman, W.C., 1993. Foundations of Probability and Statistics. Saunders College Publishing, New York, N.Y., pp. 472–474.

Sillman, S., 1995. The use of NO_x, H_2O_2, and HNO_3 as indicators for ozone-NO_x-hydrocarbon sensitivity in urban locations. Journal of Geophysical Research 100 D7, 14175–14188.

Sillman, S., He, D., Pippin, M., Daum, P.H., Lee, J.H., Kleinman, L., Weinstein-Lloyd, J., 1997. Model correlations for ozone, reactive nitrogen and peroxides for Nashville in comparison with measurements: Implications for O_3-NO_x-hydrocarbon chemistry. Journal of Geophysical Research, submitted.

Stull, R.B., 1988. An Introduction to Boundary Layer Meteorology. Kluwer Academic Publishers, Norwell, MA.

Thom, A.S., 1972. Momentum, mass, and heat exchange of vegetation. Quarternary Journal of Royal Meteorological Society 98, 124–134.

Walcek, C.J., 1987. A theoretical estimate of O_3 and H_2O_2 dry deposition over the Northeast Unites States. Atmospheric Environment 21, 2649–2659.

Wesely, M.L., Eastman, J.A., Cook, J.R., Hicks, B.B., 1978. Daytime variations of ozone fluxes to maize. Boundary Layer Meteorology 15, 361–373.

Wesely, M.L., Hicks, B.B., 1977. Some factors that affect the deposition rates of sulfur dioxide and similar gases on vegetation. Journal of Air Pollution Control Association 27 (11), 1110–1116.

Woodruff, B.L., 1986. Sampling errors in a single-instrument vertical gradient measurement in the atmospheric surface layer M.S. Thesis, Department of Atmospheric Sciences, Colorado State University, p. 79.